PERGAMON

PII: S1359-6454(98)00398-X

Acta mater. Vol. 47, No. 3, pp. 887–892, 1999

Printed in Great Britain
1359-6454/99 $19.00 + 0.00

SHAPE OF MOVING GRAIN BOUNDARIES IN Al-BICRYSTALS

J. CH. VERHASSELT[1], G. GOTTSTEIN[1]†, D. A. MOLODOV[1] and L. S. SHVINDLERMAN[2]

[1]Institut für Metallkunde und Metallphysik, RWTH Aachen, 52056 Aachen, Germany and [2]Institute of Solid State Physics, Russian Academy of Science, Chernogolovka, Moscow Distr. 142432, Russia

(Received 28 August 1998; accepted 9 November 1998)

Abstract—It is common knowledge that grain boundary migration determines microstructure evolution and thus, affects the properties of polycrystals. The principal parameter which controls the motion of a grain boundary is the grain boundary mobility. In practically all relevant cases the motion of a straight grain boundary is the exception rather than the rule. That is why the shape of a moving grain boundary is of interest, and it will be shown that the grain boundary shape is a source of new, interesting and useful findings concerning grain boundary motion, in particular for the interaction of a moving grain boundary with mobile particles. The experimentally derived shape of a grain boundary "quarter-loop" (Masteller and Bauer, *Recrystallization of Metallic Materials*, Riederer Verlag, Stuttgart, 1978) in Al-bicrystals of different purity was compared with theoretical calculations in the Lücke–Detert approximation (Lücke and Detert, *Acta metall.*, 1957, **5**, 628). *© 1999 Acta Metallurgica Inc. Published by Elsevier Science Ltd. All rights reserved.*

1. INTRODUCTION

Grain boundary mobility is the principal parameter which controls the kinetic behaviour of grain boundaries and eventually the granular microstructure of solids, its evolution during recrystallization and grain growth. The most accurate way to determine the magnitude of the grain boundary mobility is to measure it in bicrystal specimens where the characteristics of the moving grain boundary and the driving force of grain boundary motion are well defined. The most frequently used, reliable and efficient bicrystal techniques [1] are based on the observation of the steady-state motion of a curved grain boundary—so-called "half-loop" or "quarter-loop" technique. As shown recently [2], these experimental techniques are the only ones which preserve the scaling behaviour of migrating boundaries in the presence of impurities. No doubt, these techniques require a considerable experimental effort. However, these efforts are compensated for by the solid experimental data which are obtained by these techniques. Up to now, the mentioned techniques were used to measure the grain boundary mobility, whereas the information inherent in the shape of a moving grain boundary was not utilized at all.

The shape of a moving grain boundary, as mentioned above, is a new source of information. Both the orientation dependency of the grain boundary surface tension and the grain boundary mobility contribute to the grain boundary shape. Evidently, grain boundary motion manifests itself in changing the shape of the moving grain boundary. It is felt that the influence of misorientation and inclination on the thermodynamic (surface tension) and kinetic (mobility) grain boundary properties are most strongly reflected in the shape of the moving grain boundary. In the case of interactions, e.g. with solute atoms or particles, the shape changes and thus signals the interactions themselves. Therefore, the study of the grain boundary shape is an important parallel research topic in addition to the study of grain boundary mobility. In the current study we address the problem of steady-state motion of a "quarter-loop" shaped grain boundary (Fig. 1) taking into account the interaction with solute atoms or mobile particles.

2. THEORETICAL BACKGROUND

Let us consider the steady-state motion of a "quarter-loop" shaped grain boundary which is one of the most frequently used methods of grain boundary mobility measurement (Fig. 1).

In this case the steady-state motion of the grain boundary is a motion together with the line where the curved grain boundary intersects the front surface of the specimen (Fig. 1). At this front line a junction is formed by three surfaces (the grain boundary and two free surfaces) and, naturally, an equilibrium is established depending on the three corresponding surface tensions σ^B, σ_1^S and σ_2^S [3].

†To whom all correspondence should be addressed.

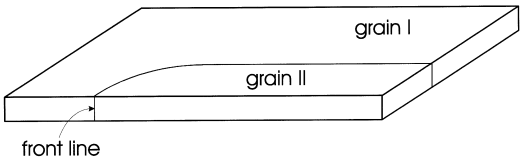

Fig. 1. Geometry of a bicrystal using the "quarter-loop" method.

Actually, the balance of the three acting forces is obeyed on the x-axis only. If we remove the condition that the shape of the surface should remain unchanged in close proximity to the front line we arrive at the equilibrium shape of this junction.

This will be addressed under the following assumptions: the front line runs straight through the sample thickness and is normal to the plane of the diagram in Fig. 2. Close to this line the grain boundary is considered to be planar. The same is also true for the two free surfaces, their planes are parallel to each other and perpendicular to the plane of the diagram. This leads to a quasi-two-dimensional problem. We further assume that the grain boundary, and thus the front line, moves under the action of the grain boundary surface tension σ^{B}. We also assume that σ^{B} and the grain boundary mobility m_{B} are independent of the orientation of the grain boundary relative to the crystallographic axes of the grains.

In this case the velocity of normal displacement for each element of a grain boundary is given by

$$v = m_{\mathrm{B}}\sigma^{\mathrm{B}}\kappa \tag{1}$$

where κ is the Laplace curvature of the considered grain boundary element. If the grain boundary moves steadily as a whole, the shape of it should be invariant, and every point moves parallel to the x-axis with velocity V, and (Fig. 3)

$$v = V\cos\varphi = V\frac{y'}{(1+(y')^2)^{1/2}} \tag{2}$$

where $y(x)$ is a function of the shape of the moving grain boundary.

Combining equations (1) and (2) and using

$$\kappa = -\frac{y''}{(1+(y')^2)^{3/2}} \tag{3}$$

leads to

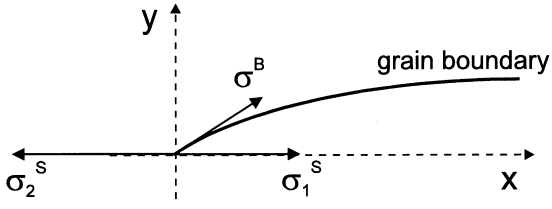

Fig. 2. Surface tensions acting on the point of the triple intersection (top view of Fig. 1).

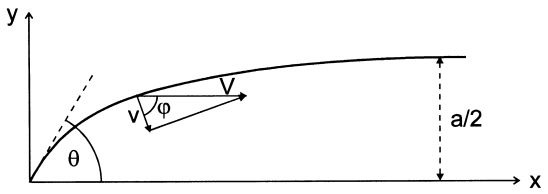

Fig. 3. Shape of a moving grain boundary using the "quarter-loop" method.

$$y'' = -\frac{V}{m_{\mathrm{B}}\sigma^{\mathrm{B}}}y'(1+(y')^2). \tag{4}$$

With the general solution of equation (4)

$$y = y_0 + \frac{m_{\mathrm{B}}\sigma^{\mathrm{B}}}{V}\arccos\left(\exp\left(-\frac{(x-x_0)V}{m_{\mathrm{B}}\sigma^{\mathrm{B}}}\right)\right) \tag{5}$$

with y_0, x_0 constants of integration and the following boundary conditions:

$$y(0) = 0 \tag{6}$$

$$y(\infty) = \frac{a}{2} \tag{7}$$

$$y'(0) = \tan\theta \tag{8}$$

the grain boundary shape is given by

$$y(x) = \frac{a}{2\theta}\left(\theta - \frac{\pi}{2}\right) + \frac{a}{2\theta}\arccos\left(\exp\left(-\frac{2\theta}{a}x + \ln(\sin\theta)\right)\right) \tag{9}$$

and according to equation (4) the grain boundary migrates with the velocity

$$V = 2\frac{\theta m_{\mathrm{B}}\sigma^{\mathrm{B}}}{a}. \tag{10}$$

Equations (9) and (10) describe the shape and the velocity of a grain boundary "quarter-loop" which moves under its own surface tension σ^{B} with its intrinsic mobility m_{B}. In other words we have not considered the fact that second phase particles or impurities in solids are not necessarily immobile. Provided they are mobile they will interact with the grain boundary, i.e. they will attach and also detach from this grain boundary [4, 5]. For a general solution this has to be taken into account.

From equation (2) it is obvious that the normal grain boundary velocity v changes locally. It is at a maximum at the front line and tends to zero where the loop section becomes parallel to the x-axis. In accordance with the theory of Lücke and Detert [6] there is a limiting velocity v^* where the segregated impurity atoms can no longer follow the grain boundary. For grain boundary sections, where the local normal grain boundary velocity v is smaller than v^*, the grain boundary does not become detached from the solute atoms and moves together with them. However, for grain boundary sections, where the local normal grain boundary velocity is

higher than v^*, the grain boundary moves detached from the impurities. Therefore, we have to distinguish two different segments of the whole grain boundary [2, 4]: one where the grain boundary moves together with the impurities, the so-called "loaded" part ($v<v^*$), and the other one where it moves detached from the segregated solute, the so-called "free" part ($v > v^*$). These parts differ in their mobilities, i.e. the mobility of the "loaded" part, m_L, will be significantly lower than that of the "free" part, m_F, or

$$0<\frac{m_L}{m_F}<1. \tag{11}$$

Related to v^* there is a point x^* on the grain boundary, which divides the grain boundary into these two segments. For $0\le x\le x^*$, $v > v^*$, and for $x\ge x^*$, $v<v^*$. As mentioned above we will use the Lücke–Detert approximation in the following.

With the corresponding constants of integration in equation (5) we obtain the general shape of the moving grain boundary for each segment introducing a substitution for the different mobilities m_F and m_L with the velocity V and the surface tension σ^B:

$$b_L = \frac{m_L\sigma^B}{V} \tag{12}$$

$$b_F = \frac{m_F\sigma^B}{V}. \tag{13}$$

Since the grain boundary cannot have kinks or discontinuities, the following conditions must be satisfied in the point x^*

$$y_L(x^*) = y_F(x^*) \tag{14}$$

$$y_L'(x^*) = y_F'(x^*). \tag{15}$$

In conjunction with the three conditions in equations (6)–(8) we can solve these five equations for the four integration constants and an expression for b_L

$$b_L = \frac{b_F\left(\arccos\left(\frac{\sin\theta}{e^{x^*/b_F}}\right)+\theta-\frac{\pi}{2}\right)-\frac{a}{2}}{\arccos\left(\frac{\sin\theta}{e^{x^*/b_F}}\right)-\frac{\pi}{2}} \tag{16}$$

which depends on b_F and x^*.

Therefore, the shape function of a moving grain boundary is described completely by

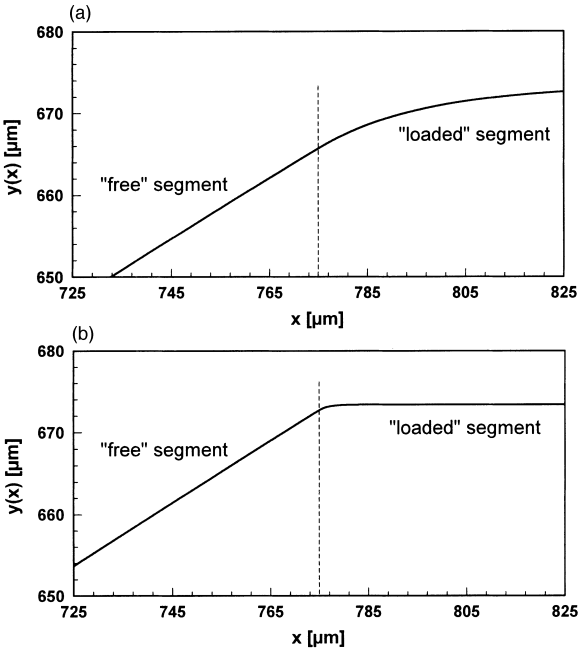

Fig. 4. Intersection of "free" and "loaded" segments of the calculated grain boundary shape: (a) $m_L/m_F = 0.0292$; (b) $m_L/m_F = 0.00245$. The dashed lines denote the position of x^*.

The parameters in equations (16) and (17) are the width $a/2$ of the shrinking grain, the angle θ of the grain boundary with the free surfaces at the front line, the critical point x^* and b_F. The first two parameters can be measured experimentally. The latter two have to be chosen in a way to fit the experimentally derived grain boundary shape.

The critical point x^* is the point of contact of the two grain boundary segments. The ratio b_L/b_F or equivalently m_L/m_F influences the grain boundary shape. The ratio of m_L/m_F is a measure of how different the shape of the "free" and the "loaded" part at the point of intersection will be. Although there is no kink or discontinuity in the calculated shape of the grain boundary at the point x^*, the change from the "free" to the "loaded" segment will be more abrupt for smaller values of m_L/m_F. To show this fact we calculate the shape with different values for m_L/m_F while holding the other parameters constant (Fig. 4).

For the larger value m_L/m_F [Fig. 4(a)] there is a very smooth transition at $x^* = 775$. For the smaller

$$y(x) = \begin{cases} -(b_F-b_L)\arccos\left(\frac{\sin\theta}{e^{x^*/b_F}}\right)+\frac{a}{2}-b_L\frac{\pi}{2}+b_F\arccos\left(\exp\left(\frac{b_F\ln(\sin\theta)-x}{b_F}\right)\right) & 0\le x\le x^* \\ \frac{a}{2}-b_L\frac{\pi}{2}+b_L\arccos\left(\exp\left(\frac{b_L\ln(\sin\theta)-x^*\left(\frac{b_L}{b_F}-1\right)-x}{b_L}\right)\right) & x\ge x^* \end{cases}. \tag{17}$$

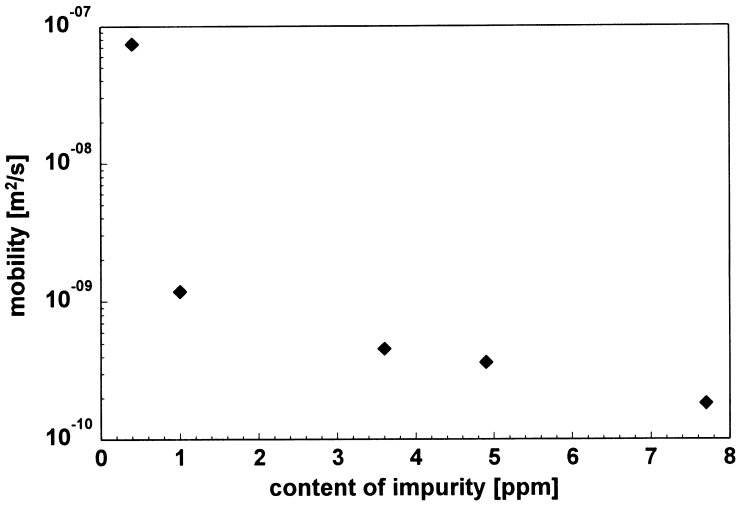

Fig. 5. Dependence of grain boundary mobility on content of impurity.

value m_L/m_F [Fig. 4(b)] this transition is not as smooth, even though there is no kink.

3. EXPERIMENTS

The calculated shape can be directly compared with the experimentally observed shape. For the experiments we used several aluminium bicrystals with 40.5° ⟨111⟩ tilt boundaries. The samples differed in the amount of solute impurities, which was determined by glow discharge mass spectrometry. We will only consider the total impurity content of each sample [7]. Bicrystals with a total impurity content of 1.0, 3.6, 4.9 and 7.7 p.p.m. were studied. Details of bicrystal growth and sample preparation are given elsewhere [8, 9]. To obtain the grain boundary mobility the velocity of grain boundary motion was measured using a specially designed X-ray device for continuous tracking of a moving grain boundary (XICTD) [10]. After the measurement of grain boundary mobility the samples were rapidly cooled to RT. Then the grain boundary shape was recorded with an image analysis system. The local resolution was about 15 μm.

The measured mobilities at a temperature of 450°C are given in Fig. 5, including a specimen with an impurity content of 0.4 p.p.m. A strong change of the mobility occurs roughly between 0.4 and 1.0 p.p.m., which is interpreted as a change of impurity content in the grain boundary. In the specimen with 0.4 p.p.m. solute atoms the grain boundary has a mobility of 7.4×10^{-8} m^2/s which can be associated with the mobility of the "free" moving grain boundary.† If the impurity content in the bicrystal is higher, the grain boundary cannot break away from the adsorbed atoms and therefore, it is forced to jointly move with its impurities. Then, the mobility is no longer determined by the intrinsic grain boundary mobility itself but by the mobility of the impurities.

To prove that there is no motion of the grain boundary without interaction with impurity atoms we used equation (9) to describe the grain boundary shape. The experimentally observed shape for the case of a 1.0 p.p.m. impurity content and the calculated shape are plotted in Fig. 6. The deviation between experimental and theoretical shape of the moving grain boundary is obvious.

For the four investigated grain boundaries the shape was calculated to fit the experimental data. In this calculation [equations (16) and (17)] we chose the value for b_F such that the respective value for m_L/m_F corresponded to the experimental value $m_F = 7.4 \times 10^{-8}$ m^2/s and m_L to the impurity content according to Fig. 5. Hence, there was only one parameter left to vary, the critical point x^*. The results are shown in Figs 7(a)–(d).

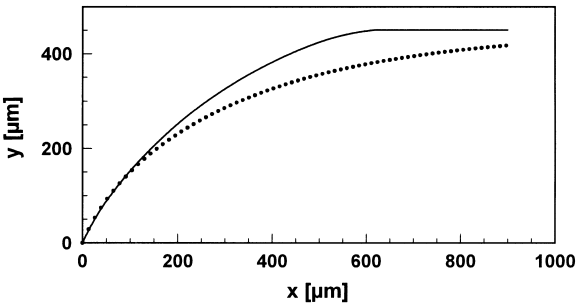

Fig. 6. Comparison between experimental data (solid line) and calculated shape (dotted line) [equation (9)].

†In this context "free" means that there is no excess of adsorbed atoms in the grain boundary in Gibbs' sense. In this case the concentration of the solute atoms in the grain boundary is not different from the concentration of the solute atoms in the bulk.

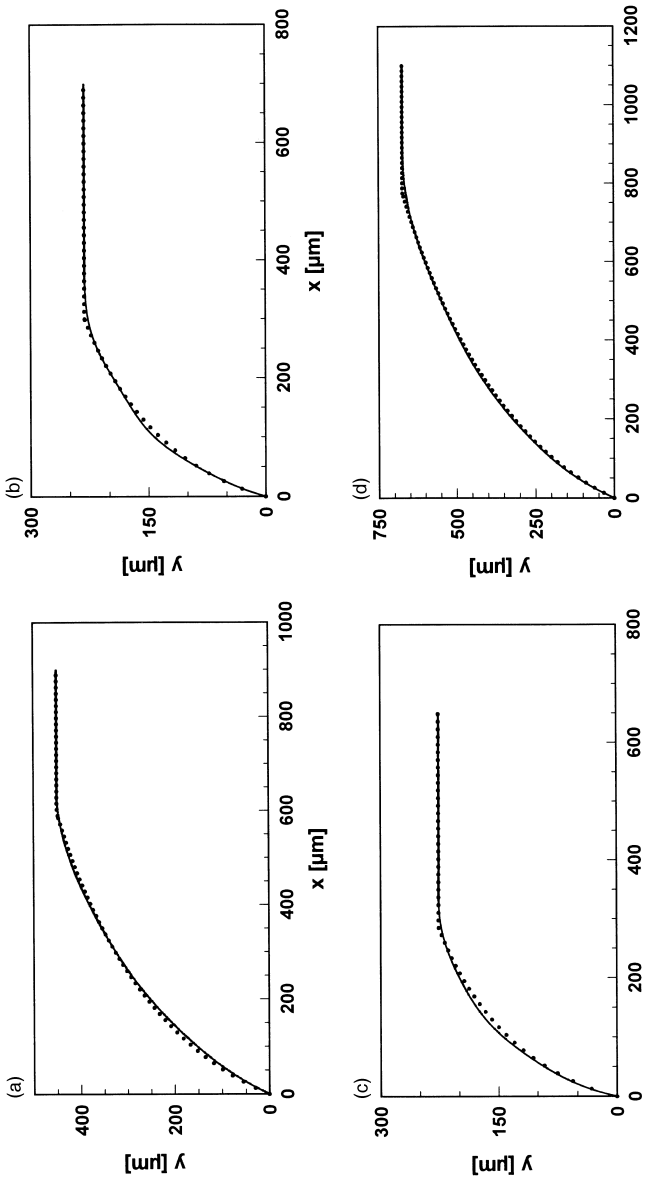

Fig. 7. Experimental (solid line) and calculated (dotted line) grain boundary shape with an impurity content of: (a) 1.0 p.p.m.; (b) 3.6 p.p.m.; (c) 4.9 p.p.m.; (d) 7.7 p.p.m.

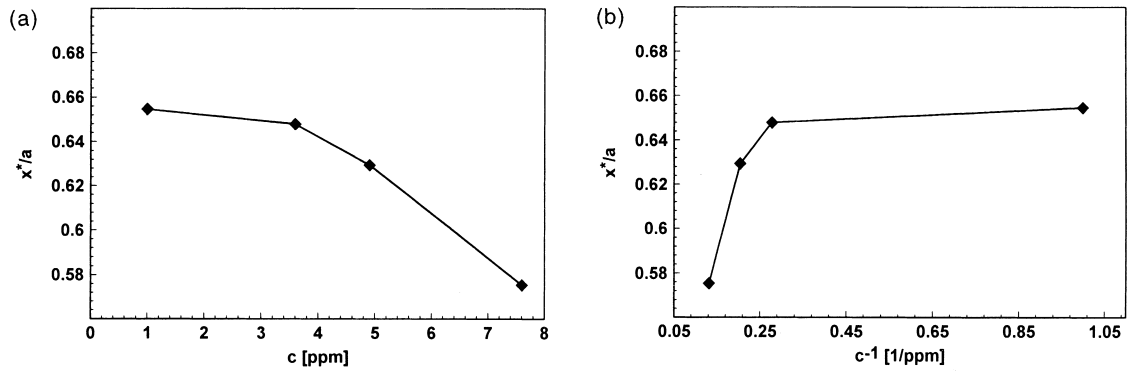

Fig. 8. Dependence of x^*/a on the impurity content c (a) and on the reciprocal impurity content c^{-1} (b).

The calculated shapes are in good agreement with the experimental data within the accuracy of measurement. The critical point x^* should be a function of the adsorption on the grain boundary and thus, it should be related to the total amount of impurities in the sample. A direct comparison of x^* for each content of impurity is not possible because of the different width of the shrinking grain in the investigated specimens and thus, a difference in driving force. But for the "quarter-loop" geometry the driving force $p = \sigma/a$ is constant. Thus, we can compare x^*/a (Fig. 8).

In theory [6, 11] v^* is supposed to vary with the adsorption and therefore, with the total amount of impurities. Correspondingly x^*/a should change in proportion to the inverse of the impurity content. While this proportionally is not confirmed experimentally (Fig. 8), in particular for larger impurity content, the trend is predicted correctly, however. This discrepancy may be due to absorption isotherms [5, 7] different from the Henry isotherm as assumed by Lücke and Detert. A larger range of concentrations will have to be investigated to settle this issue.

4. SUMMARY/CONCLUSION

The grain boundary shape was calculated for a "quarter-loop" bicrystal geometry. The theory takes into account the interaction of the grain boundary with solute atoms. In our calculations we assumed that the effect of the variation of the surface tension and the mobility due to grain boundary inclination are much smaller (in a first approximation even constant) than the variation of the mobility due to adsorbed solute atoms in the grain boundary. We used the Lücke–Detert approximation as an approach for describing the interaction with impurity atoms. In this approach the grain boundary shape can be calculated analytically, using the grain boundary mobility obtained in experiment. The calculated and experimentally observed grain boundary shapes show good agreement.

Acknowledgements—The authors would like to express their gratitude to the Deutsche Forschungsgesellschaft. One of the authors (J.Ch.V.) was financially supported by the Deutsche Forschungsgesellschaft through the "Graduiertenkolleg: Schmelze, Erstarrung. Grenzflächen".

REFERENCES

1. Masteller, M. S. and Bauer, C. L., in *Recrystallization of Metallic Materials*, ed. F. Haessner. Riederer Verlag, Stuttgart, 1978.
2. Furtkamp, M., Gottstein, G. and Shvindlerman, L. S., *Interface Sci.*, 1998, **6,** 279.
3. Antonov, A. V., Kopetskii, Ch. V., Mukovskii, Ya. M. and Shvindlerman, L. S., *Soviet Phys. Solid St.*, 1972, **13**, 2533.
4. Aristov, V. Yu., Fradkov, V. E. and Shvindlerman, L. S., *Soviet Phys. Solid St.*, 1980, **22**, 1055.
5. Gottstein, G. and Shvindlerman, L. S., *Acta metall. mater.*, 1993, **41**, 3267.
6. Lücke, K. and Detert, K., *Acta metall.*, 1957, **5**, 628.
7. Molodov, D. A., Czubayko, U., Gottstein, G. and Shvindlerman, L. S., *Acta mater.*, 1998, **46**, 553.
8. Molodov, D. A., Swiderski, J., Gottstein, G., Lojkowski, W. and Shvindlerman, L. S., *Acta metall.*, 1994, **42**, 3397.
9. Molodov, D. A., Czubayko, U., Gottstein, G. and Shvindlerman, L. S., *Scripta metall.*, 1995, **32**, 529.
10. Czubayko, U., Molodov, D., Petersen, B.-C., Gottstein, G. and Shvindlerman, L. S., *Meas. Sci. Technol.*, 1995, **6**, 947.
11. Lücke, K. and Stüwe, H. P., *Acta metall.*, 1971, **19**, 1087.